

On the saturation of the centrifugally excited curvature drift instability in AGN magnetospheres

Osmanov Z.

Georgian National Astrophysical Observatory, Ilia Chavchavadze State University

Kazbegi ave. 2^a, Tbilisi, 0160, Georgia

E-mail: z.osmanov@astro-ge.org

Abstract. We study a saturation process of the centrifugally driven curvature drift instability (CDI) in AGN magnetospheres close to the light cylinder surface to examine the twisting of magnetic field lines leading to the free motion of AGN winds, that completely kills the instability. Considering the Euler, continuity, and induction equations, by taking into account the resonant conditions, we derive the growth rate of the CDI. We show that due to the centrifugal effects, the rotational energy is efficiently pumped directly into the drift modes, that leads to the generation of a toroidal component of the magnetic field. As a result, the magnetic field lines transform into such a configuration when particles do not experience any forces and since the instability is centrifugally driven, at this stage the CDI is suspended.

PACS numbers: 98.62.Nx, 98.54.Cm, 94.20.wf, 95.30.Qd

1. Introduction

One of the fundamental problems concerning AGN relates to the understanding of a question: how the plasma goes through the light cylinder surface LCS (a hypothetical zone where the linear velocity of rigid rotation exactly equals the speed of light). It is generally believed that in AGN magnetospheres the magnetic field is strong enough to provide the frozen-in condition of plasmas, flowing in the direction of corotating field lines. On the other hand, such a dynamics of plasma particles will inevitably lead to a situation when particles' velocity achieves the speed of light on the LCS, thus violating the causality principle. Therefore, it is clear that in the mentioned zone, a certain twisting process of the magnetic field lines must exist. In [1] Rogava et al. considered curved trajectories and generalized a work developed by Machabeli and Rogava [2]. The authors examined the dynamics of a single particle, that moves along a corotating, curved channel. In this simple mechanical model the channel plays a role of magnetic field lines. It was shown that the dynamics of particles asymptotically becomes force-free if a shape of the channel is given by the Archimedes' spiral. It has been found that in the aforementioned case the particles cross the LCS without violating the causality principle.

Generally speaking, if the magnetic field is still robust, one has to twist the field lines in an appropriate way. Therefore, it is necessary to generate the toroidal component of the magnetic field provided by certain current. It is well known that particles moving along curved field lines, also drift perpendicularly to the curvature plane even if the curvature is very small. Such a drift motion creates curvature current, which leads to the necessary conditions for the development of the CDI (see e.g., [3, 4]).

The innermost region of AGN magnetospheres is supposed to be rotating, therefore, the centrifugal force (CF) seems to be essential for studying the magnetospheric plasma motion. Magneto-centrifugal effects have been extensively studied in a series of papers. In [5] the angular momentum and energy pumping process from accretion disks have been considered. The authors emphasized the special role of CF in dynamical processes governing the acceleration of plasmas. The role of the centrifugal acceleration in producing the non-thermal radiation from rotating AGN winds has been studied in [6]. We generalized this work in [7] and have shown that under certain conditions electrons might reach very high Lorentz factors 10^5 – 10^8 . The similar investigation performed for non-blazar objects was developed in [8] and the high efficiency of centrifugal acceleration was emphasized.

Generally speaking, the centrifugal acceleration may induce plasma instabilities. When the CF acts on a particle and changes with time, it plays a role of a parameter, and drives the so-called parametric instability. Centrifugally excited unstable plasma waves deserve a special interest in different astrophysical scenarios. In [9] we considered the corotating Crab magnetospheres arguing that the centrifugal force inevitably causes the separation of charges, that in turn leads to the creation of the Langmuir waves. We have shown that due to the centrifugal effects the instability is very efficient. This method was applied to AGN jets in [10] where we studied the stability problem of the rotation-induced electrostatic waves. The CF is significant also for inducing the CDI. Even if the field lines have a very small curvature, it might cause a drifting process of plasma, creating current, which will inevitably produce the toroidal component of the magnetic field. However, a value of the mentioned component is not strong enough to change a field line's configuration significantly. In this context

corotation plays an important role. Namely, as is shown in our model by means of the centrifugal acceleration, the rotational energy can be pumped directly into the toroidal component, amplifying it efficiently. This is the meaning of the curvature drift instability. For examining the role of the corotation in the curvature drift instability for pulsar magnetospheres, in [11] we studied the two-component relativistic plasma, estimating the increment of the instability. We have found that the growth rate was bigger than pulsar's spin-down rates by many orders of magnitude, indicating high efficiency of the CDI. This instability is very important since, due to the mentioned drift, current is produced, which, via the parametric mechanism leads to the creation of the amplifying toroidal magnetic field, reconstructing the magnetosphere. By the influence of the toroidal magnetic field, the initial field lines are twisting until they transform into the shape of the Archimedes spiral, when the motion of the particles is described by the so-called force-free regime [12].

In the present paper we investigate the saturation (transition) mechanism of the CDI in AGN winds.

The paper is arranged as follows. In Sect. 2, we introduce the curvature drift waves and derive the dispersion relation and a corresponding expression of the transition timescale. In Sect. 3, the results for typical AGN are presented and, in Sect. 4, we summarize our results.

2. Excitation of curvature drift waves

We consider plasma that consists of relativistic electrons with the Lorentz factor $\gamma \sim 10^{5-8}$ [7], [8]. It is assumed that the field lines initially are almost rectilinear and corotate. As we have already mentioned in the introduction, current providing the twisting of field lines is created due to the curvature drift, characterized by the following (curvature drift) velocity

$$u = \frac{\gamma_0 v_{\parallel}^2}{\omega_B R_B}, \quad (1)$$

where $\omega_B = eB_0/mc$, e and m are particle's charge and the rest mass respectively, B_0 is the unperturbed magnetic induction, c is the speed of light, R_B is the curvature radius of magnetic field lines, γ_0 is the initial Lorentz factor of particles and v_{\parallel} is the longitudinal velocity. As is clear from Eq. (1), the drift velocity is proportional to $\gamma_0 m$, therefore, the corresponding value of the bulk flow (protons) (having the Lorentz factor of the order of 10), will be by many orders of magnitude less than that of the relativistic electrons (with $\gamma_0 \sim 10^{5-8}$). This in turn means that the contribution of protons is negligible and we consider one-component plasma composed of relativistic electrons.

In the zeroth approximation particles move along the magnetic field lines and our aim is to consider the twisting process of these field lines and study a subsequent saturation mechanism.

For studying the development of the CDI we consider the Euler equation, which governs the dynamics of corotating plasma particles [13]

$$\frac{\partial \mathbf{p}}{\partial t} + (\mathbf{v} \cdot \nabla) \mathbf{p} = -c^2 \gamma \xi \nabla \xi + \frac{e}{m} \left(\mathbf{E} + \frac{1}{c} \mathbf{v} \times \mathbf{B} \right), \quad (2)$$

where

$$\xi \equiv \sqrt{1 - \Omega^2 R^2 / c^2},$$

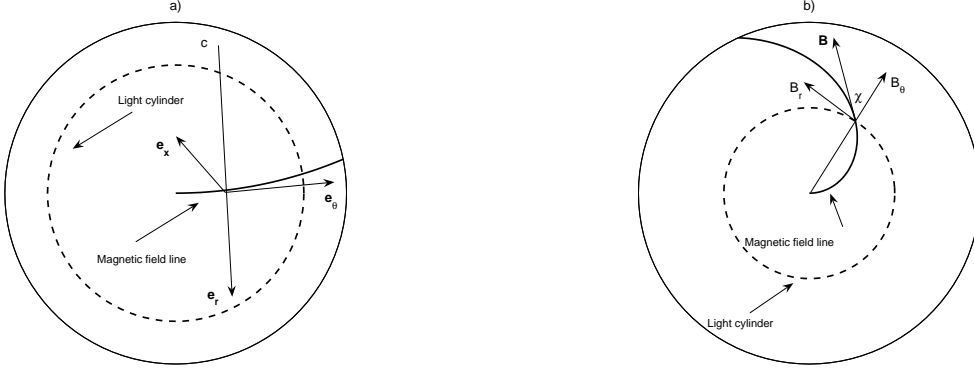


Figure 1. a) The geometry in which the set of main Eqs. (2-4) is considered; $(\mathbf{e}_\theta, \mathbf{e}_r, \mathbf{e}_x)$ denotes orthonormal basis of unit vectors; \mathbf{e}_x is directed perpendicularly to the plane of the figure (equatorial plane); C is the center of the curvature; and \mathbf{e}_θ and \mathbf{e}_r are the tangential and perpendicular (with respect to the field line) unit vectors respectively. b) The geometry for deriving Eq. (26): the curved line denotes the twisted magnetic field, \mathbf{B} , generated due to the raising of magnetic perturbation, \mathbf{B}_r . Note, that \mathbf{B}_r and \mathbf{B}_θ are oriented with respect to the initial ‘quasi straight’ magnetic field line.

and \mathbf{p} is the momentum, \mathbf{v} is the velocity, γ is the Lorentz factor of the relativistic particles, and \mathbf{E} and \mathbf{B} are the electric field and the magnetic induction, respectively. Ω is the angular velocity of rotation and R is the coordinate along the magnetic field lines. We express the equation of motion in the cylindrical coordinates (see Fig. 1a). The first term on the right-hand side of the Euler equation $-c^2\gamma\xi\nabla\xi$ represents the centrifugal force. As we see, this force becomes infinity on the LCS, therefore, its overall effect is significant in the mentioned zone. For closing the system, we add to Eq. (2) the continuity equation:

$$\frac{\partial\rho}{\partial t} + \nabla \cdot \mathbf{J} = 0, \quad (3)$$

and the induction equation:

$$\nabla \times \mathbf{B} = \frac{1}{c} \frac{\partial \mathbf{E}}{\partial t} + \frac{4\pi}{c} \mathbf{J}, \quad (4)$$

respectively. By $\rho \equiv en$ and $\mathbf{J} \equiv en\mathbf{v}$ we denote the charge density and the current density, respectively and n represents the electron density.

If we take into account the frozen-in condition, $\mathbf{E}_0 + \mathbf{v}_0 \times \mathbf{B}_0/c = \mathbf{0}$, describing the leading state of the system, then one can show that Eq. (2) reduces to [2]:

$$\frac{dv}{dt} = \frac{\Omega^2 R}{1 - \frac{\Omega^2 R^2}{c^2}} \left[1 - \frac{\Omega^2 R^2}{c^2} - \frac{2v^2}{c^2} \right]. \quad (5)$$

For the ultra relativistic case ($\gamma \gg 1$) and the following initial conditions: $R(0) = 0$, $v(0) \approx c$ ($v \equiv dR/dt$) a solution to Eq. (5) is given by

$$v(t) \equiv v_{\parallel} \approx c \cos(\Omega t + \varphi), \quad (6)$$

where φ denotes the initial phase of a particle.

As we have already mentioned above, we assume that the magnetic field lines initially have a small curvature, that drives the particles along the x axis (see Fig.

1a). The mentioned drift causes current, which in turn creates the toroidal component of the magnetic field.

For studying the development of the CDI we linearize the system of equations in Eqs. (2-4), by expanding all physical quantities around the leading state

$$\Psi \approx \Psi^0 + \Psi^1, \quad (7)$$

$$\Psi = \{n, \mathbf{v}, \mathbf{p}, \mathbf{E}, \mathbf{B}\}, \quad (8)$$

where the zeroth order quantities are given by $n_0 = \text{const}$, $v_{0x} = u$, $v_{0\theta} = v_{\parallel}$, $\mathbf{p}_0 = \mathbf{v}_0/\gamma_0$, $B_{0\theta} = B_0$ (see below equation (13)), $B_{0r} = B_{0x} = 0$, $\mathbf{E}_0 = -\mathbf{v}_0 \times \mathbf{B}_0/c$

We then express the perturbed quantities as

$$\Psi^1(t, \mathbf{r}) \propto \Psi^1(t) \exp[i(\mathbf{k}\mathbf{r})], \quad (9)$$

which reduces the set of equations in Eqs. (2-4) to

$$\frac{\partial p_x^1}{\partial t} - i(k_x u + k_{\theta} v_{\parallel}) p_x^1 = \frac{e}{mc} v_{\parallel} B_r^1, \quad (10)$$

$$\frac{\partial n^1}{\partial t} - i(k_x u + k_{\theta} v_{\parallel}) n^1 = i k_x n^0 v_x^1, \quad (11)$$

$$-i k_{\theta} c B_r^1 = 4\pi e (n^0 v_x^1 + n^1 u), \quad (12)$$

where k_x and k_{θ} are the wave vector components corresponding to the coordinate system described in Fig. (1a). By

$$B_0 = \sqrt{\frac{2L}{R_c c^2}} \quad (13)$$

we denote the equipartition magnetic induction on the LCS for the leading state, (where L is the luminosity of AGN and $R_c = c/\Omega$ is the light cylinder radius). In deriving Eqs. (10-12), the wave propagating almost perpendicular to the equatorial plane, was considered and the expression $v_r^1 \approx cE_x^1/B_0$ was taken into account. For simplicity, the set of equations are given in terms of the coordinates of the field line (see Fig. 1a).

Introducing a special ansatz for v_x^1 and n^1

$$v_x^1 \equiv V_x e^{i\mathbf{k}\mathbf{A}(t)}, \quad (14)$$

$$n^1 \equiv n e^{i\mathbf{k}\mathbf{A}(t)}, \quad (15)$$

where

$$A_x(t) = \frac{ut}{2} + \frac{u}{4\Omega} \sin[2(\Omega t + \varphi)], \quad (16)$$

$$A_{\phi}(t) = \frac{c}{\Omega} \sin(\Omega t + \varphi), \quad (17)$$

and by substituting Eqs. (14) and (15) into Eqs. (10-12), it is straightforward to solve the system for the toroidal component

$$\begin{aligned} -i k_{\phi} c B_r^1(t) &= \frac{\omega_e^2}{\gamma_{e0}} e^{i\mathbf{k}\mathbf{A}(t)} \int^t e^{-i\mathbf{k}\mathbf{A}(t')} v_{\parallel}(t') B_r(t') dt' + \\ & i \frac{\omega_e^2}{\gamma_{e0}} k_x u e^{i\mathbf{k}\mathbf{A}(t)} \int^t dt' \int^{t''} e^{-i\mathbf{k}\mathbf{A}(t'')} v_{\parallel}(t'') B_r(t'') dt'' \end{aligned}$$

(18)

where $\omega_e = e\sqrt{4\pi n_{e0}/m}$ and n_{e0} are the plasma frequency and initial electron density respectively. To simplify Eq. (18), one may use the following identity

$$e^{\pm ix \sin y} = \sum_s J_s(x) e^{\pm isy}, \quad (19)$$

where $J_s(x)$ ($s = 0; \pm 1; \pm 2 \dots$) is the Bessel function of integer order [14]. Eq. (18) then reduces to

$$\begin{aligned} B_r(\omega) = & -\frac{\omega_e^2}{2\gamma_{e0}k_{\theta}c} \sum_{\sigma=\pm 1} \sum_{s,q,l,p} \frac{J_s(g)J_q(h)J_l(g)J_p(h)}{\omega + \frac{k_x u}{2} + \Omega(2s+q)} \times \\ & \times B_r(\omega + \Omega(2[s-l] + q - p + \sigma)) \left[1 - \frac{k_x u}{\omega + \frac{k_x u}{2} + \Omega(2s+q)} \right] \times \\ & \times e^{i\varphi(2[s-l]+q-p+\sigma)} + \\ & + \frac{\omega_e^2 k_x u}{4\gamma_{e0}k_{\theta}c} \sum_{\sigma,\mu=\pm 1} \sum_{s,q,l,p} \frac{J_s(g)J_q(h)J_l(g)J_p(h)}{\left(\omega + \frac{k_x u}{2} + \Omega(2[s+\mu] + q)\right)^2} \times \\ & \times B_r(\omega + \Omega(2[s-l+\mu] + q - p + \sigma)) \times e^{i\varphi(2[s-l+\mu]+q-p+\sigma)}, \quad (20) \end{aligned}$$

where

$$g = \frac{k_x u}{4\Omega}, \quad h = \frac{k_{\theta} c}{\Omega}.$$

For solving Eq. (20) we must examine similar expressions, by rewriting Eq. (20) for the infinite number of components $B_r(\omega \pm \Omega)$, $B_r(\omega \pm 2\Omega)$,... etc. Therefore, the system becomes composed of the infinite number of equations, that makes the task unsolvable. To overcome this problem we use a physically reasonable cutoff on the-right hand side of the equation [15]. As is clear from Eq. (20), the considered instability is characterized by proper frequency of the curvature drift modes

$$\omega_0 \approx -\frac{k_x u}{2}, \quad (21)$$

when the corresponding conditions $k_x u/2 < 0$, $2s + q = 0$, and $2[s + \mu] + q = 0$ are satisfied. As we see, only the resonance terms provide a significant contribution to the result.

We consider the typical parameters for AGN magnetospheres $L \sim 10^{44} \text{ erg/s}$, $\Omega = 3 \times 10^{-5} \text{ s}^{-1}$, $\gamma_{e0} \sim 10^5$, $R_B \approx R_{lc}$, $n_{e0} \sim 0.001 \text{ cm}^{-3}$. Then, one can show that for the curvature drift waves with the wavelength $\lambda \sim R_{lc}$ ($\lambda = 2\pi/k$). For making the physics realistic we have assumed that $k_x < 0$ and $u > 0$, otherwise the frequency becomes negative) one has the following relation $|k_x u/2| \sim 10^{-12} \text{ s}^{-1} \ll \Omega$. Therefore, all terms with non-zero values of $\Omega(2s+q)$ and $\Omega(2[s+\mu]+q)$ oscillate rapidly and therefore do not contribute to a final result.

Since particles have different phases, to solve Eq. (20), we must examine the average value of B_r with respect to φ . Then, by taking into account the formula

$$\frac{1}{2\pi} \int e^{iN\varphi} d\varphi = \delta_{N,0},$$

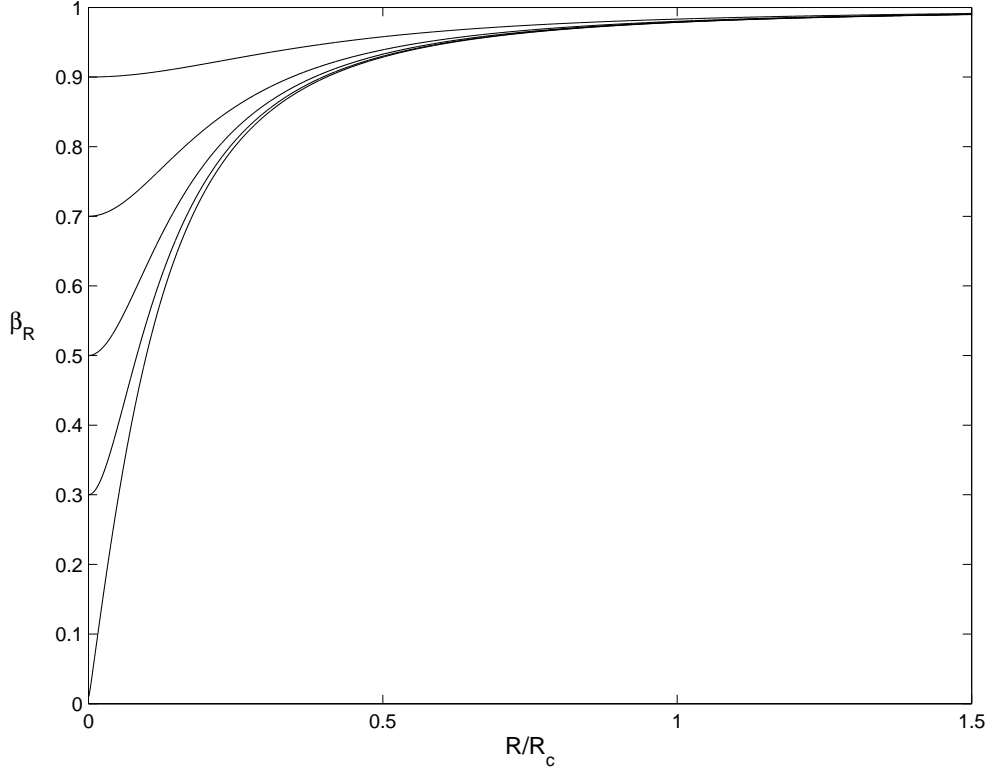


Figure 2. Behaviour of β_R versus R/R_c . The set of parameters is $\beta_{R0} = \{0.01; 0.3; 0.5; 0.7; 0.9\}$.

after preserving only the leading terms the dispersion relation of the CDI is given by [11]

$$\left(\omega + \frac{k_x u}{2}\right)^2 \approx \sum_{\sigma, \mu = \pm 1} \sum_{s, l} \Xi_\mu J_s(g) J_{q'(s, \mu)}(h) J_l(g) J_{p'(l, \sigma)}(h), \quad (22)$$

where

$$\Xi_0 = 2\Xi_{\pm 1} = \frac{\omega_e^2 k_x u}{2\gamma_{e0} k_\theta c}, \quad (23)$$

$$q' = -2(s + \mu), \quad p' = -2l + \sigma.$$

To determine the CDI growth rate, Γ , let us write $\omega \equiv \omega_0 + i\Gamma$ and substitute this into Eq. (22). Then, it is easy to show that the increment gets the following form

$$\Gamma \approx \left[\sum_{\sigma, \mu = \pm 1} \sum_{s, l} \Xi_\mu J_s(g) J_{-2(s + \mu)}(h) J_l(g) J_{-2l + \sigma}(h) \right]^{\frac{1}{2}}. \quad (24)$$

It is worth noting that this instability is unavoidable for plasma magnetospheric flows, because for the developing of the ICS a) the initial curvature should be

nonzero and b) the magnetic field must be robust enough to provide the frozen-in condition. (a)-is a necessary condition for creating the drift waves and (b)-guarantees the parametric mechanism of rotational energy pumping directly into the drift modes.

3. Discussion

Let us consider the Archimedes' spiral $\Phi = aR$, where Φ and R are the polar coordinates and $a = \text{const}$. As was shown in [1] if the particle slides along the rotating channel that has the shape of the Archimedes' spiral then, an observer from the laboratory frame of reference will measure the effective angular velocity $\Omega_{ef} = \Omega + d\Phi/dt = \Omega + av$, where v is the longitudinal velocity of a particle. If the particle moves without acceleration in the laboratory frame of reference, the corresponding effective angular velocity must be equal to zero ($\Omega_{ef} = 0$). Therefore, $v = v_c \equiv -\Omega/a$ which means that, for any Archimedes' spiral with $a < -\Omega/c$, the dynamics of the particle becomes force-free and the particle moves with a certain "characteristic velocity", v_c .

After defining the corresponding components of the relativistic momentum $P_R = \gamma mv$, $P_\Phi = \gamma mR\Omega_{ef}$, the equation of motion, $d\mathbf{P}/dt = \mathbf{F}$ (\mathbf{F} is the reaction force), leads to the following equation [1]

$$\frac{d^2 R}{dt^2} = \frac{\Omega - \gamma^2 v(a + \Omega v/c^2)}{\gamma^2 \kappa^2} \Omega_{ef} R, \quad (25)$$

where

$$\kappa \equiv \left(1 - \frac{\Omega^2 R^2}{c^2} + a^2 R^2 \right)^{1/2}.$$

We note that $(d^2 R/dt^2) \equiv 0$, when $v = v_c = -\Omega/a$.

Typical AGN outflows are highly relativistic, therefore, let us consider $v_c \approx c$ setting $a = -\Omega/c$. In Fig. 2, we plot the solution to Eq. (25), that is the dependence of $\beta_R \equiv v/c$ versus R/R_c (R_c is the light cylinder radius) for different initial values of β_{R0} . As is clear from these plots, no matter what is the initial velocity of the particle, it asymptotically converges to the characteristic velocity, v_c . This implies that the dynamics of the particle asymptotically becomes force-free.

Now we can qualitatively analyze how the configuration of magnetic field lines changes with time. After perturbing the magnetic field in the transverse direction, the toroidal component will amplify. As a result the field lines will gradually lag behind the rotation. On the other hand, for the twisted field lines, their dynamical influence on particles will decrease. In the parallel regime, the efficiency of the CDI will also decrease and when the field lines get a shape of the Archimedes' spiral the instability completely vanishes since the CDI is centrifugally driven and as we see from Eq. (25) the radial acceleration becomes vanishing for this case. Therefore at this stage our aim is to estimate from Eq. (24) the timescale of transition of quasi-straight field lines into the Archimedes' spiral, in other words we have to estimate a characteristic time of saturation of the CDI.

Let us assume that when the particle dynamics becomes force-free, the critical value of the toroidal magnetic field is B_r , then referring to Fig. 1b, one can show that $\tan \chi = B_r/B_\theta$. If we apply the exponential temporal behaviour of the toroidal component, $B_r \approx B_r^0 \exp(\Gamma\tau)$, then the corresponding transition timescale gets the

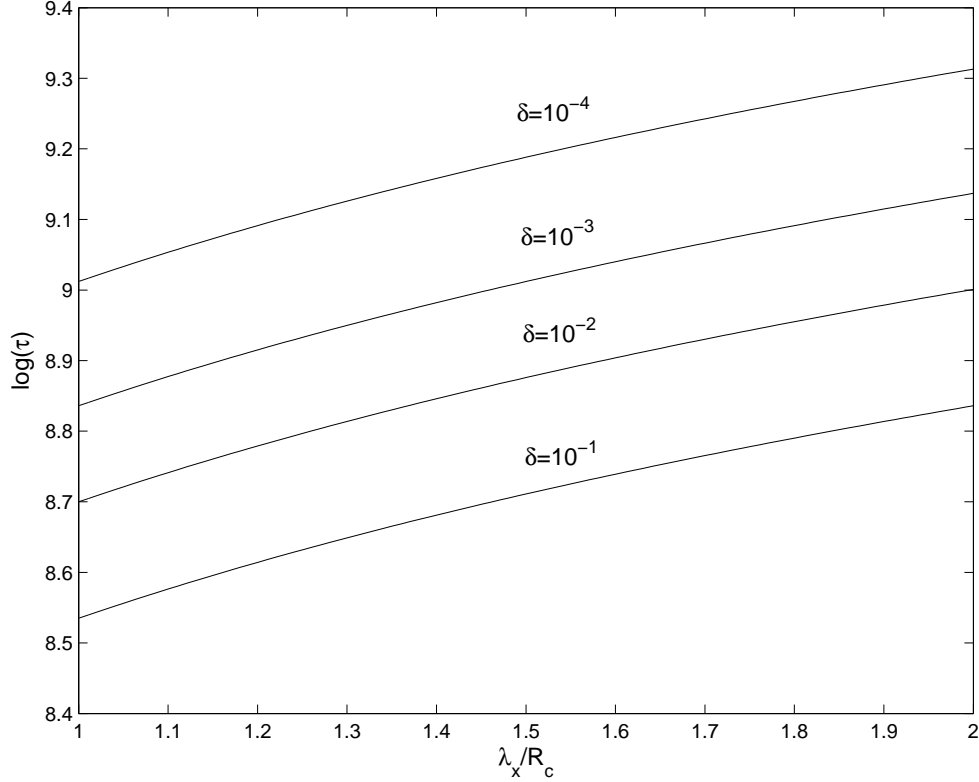


Figure 3. The dependence of logarithm of the transition timescale on the normalized wavelength. The set of parameters is $\Omega = 3 \times 10^{-5} s^{-1}$, $L/L_E = 0.01$, $\delta \in \{10^{-1}; 10^{-2}; 10^{-3}; 10^{-4}\}$, $\gamma_{e0} = 10^8$, $R_B \approx R_c$, $n_{e0} = 0.001 cm^{-3}$ and $\lambda_\theta \equiv 2\pi/k_\theta = 100R_c$.

form

$$\tau \approx -\frac{1}{\Gamma} \ln \left(\frac{B_r^0}{B_\theta} \right). \quad (26)$$

We have taken into account that for the considered Archimedes' spiral ($a = -\Omega/c$), $\tan \chi = 1$. Generally speaking, the role of the CDI is twofold. At the one hand it guarantees the required twisting of magnetic field lines, and at the other hand, in terms of its feedback on plasma dynamics it provides necessary conditions for the saturation process.

We consider the behaviour of the transition timescale versus the wavelength of the perturbation and the AGN bolometric luminosity respectively. For this purpose let us examine the typical AGN parameters: $M_{BH} = 10^8 \times M_\odot$, $\Omega = 3 \times 10^{-5} s^{-1}$ and $L = 10^{44} erg/s$, where M_{BH} represents the AGN mass, M_\odot is the solar mass and L is the bolometric luminosity.

In Fig. 3 we show the logarithm of the saturation timescale versus the wavelength normalized to the light cylinder radius for different values of initial perturbation $B_r^0/B_\theta \equiv \delta \in \{10^{-1}; 10^{-2}; 10^{-3}; 10^{-4}\}$. The set of parameters is $\Omega = 3 \times 10^{-5} s^{-1}$, $L/L_E = 0.01$, $\gamma_{e0} = 10^8$, $R_B \approx R_c$, $n_{e0} = 0.001 cm^{-3}$ and $\lambda_\theta \equiv 2\pi/k_\theta = 100R_c$, where

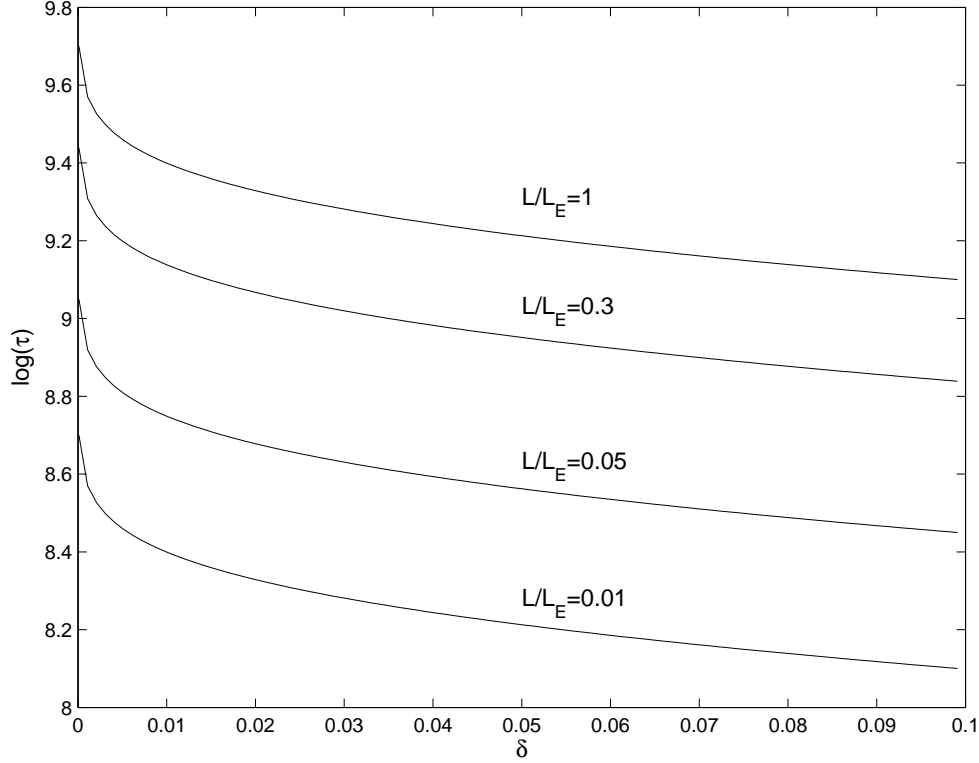


Figure 4. The dependence of logarithm of the transition timescale on the dimensionless perturbation. The set of parameters is $\Omega = 3 \times 10^{-5} s^{-1}$, $L/L_E = \{0.01; 0.05; 0.3; 1\}$, $\gamma_{e0} = 10^8$, $R_B \approx R_c$, $n_{e0} = 0.001 cm^{-3}$, $\lambda_\theta \equiv 2\pi/k_\theta = 100R_c$ and $\lambda_x = R_c$.

$L_E = 10^{46} erg/s$ is the Eddington luminosity for the given AGN mass. By different curves we show different cases of initial perturbation. As we see from the plots, the timescale is a continuously increasing function of $\lambda_x (\equiv 2\pi/k_x)$. Indeed, from Eq. (23) we get $\Xi_{0,\pm 1} \sim 1/\lambda_x$, which combining with Eq. (26) provides $\tau \propto \sqrt{\lambda_x}$. As a result, for the parameters considered in Fig. 3, the transition timescale varies from $\sim 10^8 s$ ($\lambda_x/R_c = 1$, $\delta = 10^{-1}$) to $\sim 10^9 s$ ($\lambda_x/R_c = 2$, $\delta = 10^{-4}$).

In Fig. 4, we display the behaviour of $\log(\tau)$ versus the initial perturbation for different values of luminosities. The set of parameters is $\Omega = 3 \times 10^{-5} s^{-1}$, $L/L_E = \{0.01; 0.05; 0.3; 1\}$, $\gamma_{e0} = 10^8$, $R_B \approx R_c$, $n_{e0} = 0.001 cm^{-3}$, $\lambda_\theta \equiv 2\pi/k_\theta = 100R_c$ and $\lambda_x = R_c$. The figure shows the continuously decreasing behaviour of the transition timescale. This is a natural consequence of the fact that for bigger perturbations one needs lower time to reach the critical value B_r . On the other hand as we see from the plots, the instability is less efficient (bigger timescale) for more luminous AGN. Such a behaviour is clearly seen from an expression of the drift velocity in Eq. (1). Indeed, as we see, the drift velocity is proportional to the inverse value of the cyclotron frequency, which is bigger for bigger magnetic fields. On the other hand, from Eq. (13) we have $B_0 \propto \sqrt{L}$, which means that the curvature drift velocity is proportional

to $1/\sqrt{L}$. Since the curvature drift waves are more efficient for bigger curvature drift velocities, by increasing the bolometric luminosity, the increment of the instability will inevitably decrease and the corresponding transition timescale will be bigger. For the parameters used for Fig. 4 the transition timescale varies from $\sim 10^{10}s$ ($\delta = 10^{-4}$, $L/L_E = 1$) to $\sim 10^8s$ ($\delta = 10^{-1}$, $L/L_E = 0.01$).

Summarizing our results we see that the saturation timescale lies in the range: $\tau \in \{10^8; 10^{10}\}s$. A next step is to specify how efficient the twisting of field lines is. For this purpose it is relevant to examine an accretion process on AGN, estimate the corresponding evolution timescale, and compare with that of the saturation.

Since the accretion is related to the self gravitating mass, M_{sg} , King & Pringle considering fuelling of AGN, showed in [16] that M_{sg} is given by

$$M_{sg} = 2.76 \times 10^5 \left(\frac{\eta}{0.03} \right)^{-2/27} \left(\frac{\epsilon}{0.1} \right)^{-5/27} \left(\frac{L}{0.1L_E} \right)^{5/27} \times \left(\frac{M_{BH}}{10^8 M_\odot} \right)^{23/27} M_\odot, \quad (27)$$

where η is the Shakura-Sunyaev viscosity parameter [17] and ϵ is the accretion parameter related to the accretion mass rate \dot{M} and the bolometric luminosity

$$\epsilon \equiv \frac{L}{\dot{M}c^2}. \quad (28)$$

By defining the accretion timescale to be $t_{evol} \equiv M_{sg}/\dot{M}$ one can show that [16]

$$t_{evol} = 3.53 \times 10^{13} \left(\frac{\eta}{0.03} \right)^{-2/27} \left(\frac{\epsilon}{0.1} \right)^{22/27} \left(\frac{L}{0.1L_E} \right)^{-22/27} \times \left(\frac{M_{BH}}{10^8 M_\odot} \right)^{-4/27} s. \quad (29)$$

From this expression is clear that the evolution timescale varies from $\sim 10^{12}s$, ($M_9 = 1$ and $L/L_E = 1$), to $\sim 10^{15}s$ ($M_9 = 0.001$ and $L/L_E = 0.01$), where $M_9 \equiv M_{BH}/(10^9 \times M_\odot)$. If one compares these timescales with that of the transition, one finds that t_{evol} exceeds τ by many orders of magnitude, illustrating the high efficiency of the curvature drift instability.

We have shown that the saturation of the CDI is extremely efficient, however, it is worth noting that the twisting process of magnetic field lines requires a certain amount of energy and a natural question arises: is the energy budget enough to provide the aforementioned process?.

Let us introduce the maximum value of the possible AGN luminosity $L_{max} = \dot{M}c^2$ and compare this with the "luminosity" corresponding to the twisting of the magnetic field lines $L_m \equiv \Delta E_m / \Delta t \approx \Delta E_m / \tau$. ΔE_m is the variation in the magnetic energy due to the curvature drift instability.

We consider AGN with $L = 10^{45} \text{ erg/s}$, then, assuming $\epsilon = 0.1$, one can show from Eq. (28) that

$$L_{max} = 10^{46} \text{ erg/s}. \quad (30)$$

If the reconstruction of the magnetosphere is feasible, then one has to satisfy the condition $L_m < L_{max}$. The magnetic "luminosity" can be estimated straightforwardly

$$L_m = \frac{B_r^2}{4\pi\tau} R_c^3 \kappa. \quad (31)$$

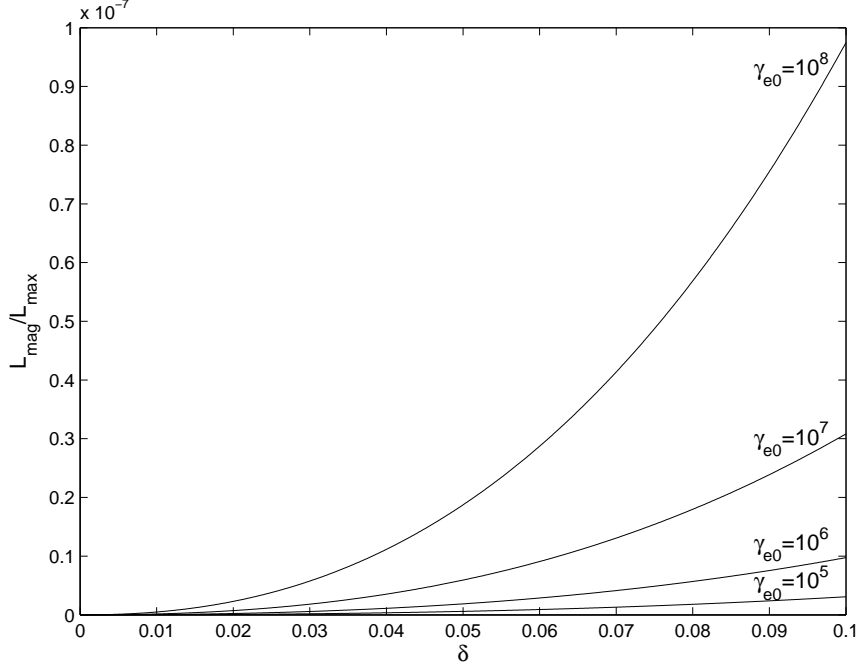


Figure 5. The dependence of L_m/L_{max} versus δ . The set of parameters is $\Omega = 3 \times 10^{-5} s^{-1}$, $L = 10^{45} erg/s$, $\gamma_{e0} = \{10^5; 10^6; 10^7; 10^8\}$, $R_B \approx R_c$, $n_{e0} = 0.001 cm^{-3}$, $\lambda_\theta = 100 R_c$ and $\lambda_x = R_c$.

where $\Delta V \approx R_c^2 \Delta R = R_c^3 \kappa$ ($\kappa \equiv \Delta R/R_c \ll 1$) is the volume, where the twisting process takes place and B_r behaves as

$$B_r = B_r^0 e^{t/\tau}, \quad (32)$$

where B_r^0 is the initial perturbation of the toroidal component.

Let us consider the following set of parameters $\gamma_{e0} = \{10^5; 10^6; 10^7; 10^8\}$, $R_B \approx R_c$, $n_{e0} = 0.001 cm^{-3}$, $\lambda_\phi = 100 R_c$, $\lambda_x = R_c$ and $L = 10^{45} erg/s$. In Fig. 5 we plot the behaviour of L_m/L_{max} versus the initial perturbation for the moment of the transition ($t \approx \tau$). Different curves correspond to different Lorentz factors. As is clear from Fig. 5, the total luminosity budget, exceeds, by many orders of magnitude, the magnetic luminosity, indicating that this process is feasible.

4. Summary

We summarize the principal steps and conclusions of our study to be:

- (i) We have studied the centrifugally driven curvature drift instability and the corresponding saturation process for AGN magnetospheres.
- (ii) By linearizing the Euler, continuity and induction equations we have derived the dispersion relation of the parametrically excited curvature drift instability and obtained an expression of the growth rate for the light cylinder area.

- (iii) As a next step we have estimated the transition timescale of quasi-linear configuration of magnetic field lines into the Archimedes spiral. Such a shape of field lines guarantees the force-free dynamics of particles and necessarily provides the saturation of the instability.
- (iv) We have shown that the transition timescale was lower by many orders of magnitude than the accretion evolution timescale, illustrating extremely high efficiency of the CDI.
- (v) Analyzing the energy budget, it has been shown that the reconstruction of the magnetic field lines requires only a tiny fraction of the total energy budget, indicating that the CDI is a working process.

In the present paper we imposed several restrictions. Namely, we described the plasma dynamics based on a single particle approach. Although it is natural to suppose that the collective phenomena may influence the process of the development of the curvature drift instability and a generalization of the present model to a more realistic astrophysical scenario is needed.

In this paper we considered the magnetic field lines located in the equatorial plane. However, in realistic astrophysical cases, the magnetic field lines also might have poloidal components. Therefore, to extend the approach, it is essential to study the CDI for a general configuration of the magnetic field.

Acknowledgments

I thank professor G. Machabeli for valuable discussions. The research was supported by the Georgian National Science Foundation grant GNSF/ST06/4-096.

References

- [1] Rogava A. D., Dalakishvili G. & Osmanov Z., 2003, *Gen. Rel. and Grav.* 35, 1133
- [2] Machabeli G. & Rogava A. D., 1994, *Phys.Rev. A*, 50, 98
- [3] Kazbegi A.Z., Machabeli G.Z. & Melikidze G.I., 1991, *Mon. Not. R. Astron. Soc.*, 253, 377
- [4] Shapakidze, D., Machabeli, G. Melikidze, G., & Khechinashvili, D., 2003, *Phys.Rev.E*, 67, 026407
- [5] Blandford, R. D., & Payne, D. G., 1982, *Mon. Not. R. Astron. Soc.*, 199, 883
- [6] Gangadhara R.T., Lesch H. 1997, *Astron. Astrophys.*, 323, L45
- [7] Osmanov Z., Rogava A.S. & Bodo G., 2007, *Astro. Astrophys.*, 470, 395
- [8] Rieger F. M. & Aharonian F. A., 2008, *Astron. Astrophys.*, 479, 5
- [9] Machabeli G., Osmanov Z. & Mahajan S., 2005, *Phys. Plasmas* 12, 062901
- [10] Osmanov Z., 2008, *Phys. Plasmas*, 15, 032901
- [11] Osmanov Z., Dalakishvili Z. & Machabeli Z. 2008a, *Mon. Not. R. Astron. Soc.*, 383, 1007
- [12] Osmanov Z., Shapakidze D. & Machabeli G., 2008b, *Astron. Astrophys.*, 503, 19
- [13] Chedia O.V., Kahnashvili T.A., Machabeli G.Z. & Nanobashvili I.S., 1996, *Astrophys. Space Sci.* 239, 57.
- [14] Abramovitz, M. & Stegun, I., 1965, *Handbook of Mathematical Functions*, (eds.: Dover Publications Inc.: New York), p. 320
- [15] Silin V.P. & Tikhonchuk V.T., 1970, *J. Appl. Mech. Tech. Phys.*, 11, 922
- [16] King A. R. & Pringle J. E., 2007, *Mon. Not. R. Astron. Soc.*, 377, 25
- [17] Shakura N. I. & Sunyaev R. A., 1973, *Astron. Astrophys.*, 24, 337